

Electronic structure and magnetic anisotropy of CrO_2

A. Toropova and G. Kotliar

Center for Materials Theory, Department of Physics and Astronomy, Rutgers University, Piscataway, NJ 08854

S. Y. Savrasov

Department of Physics, New Jersey Institute of Technology, Newark, NJ 07102

V. S. Oudovenko

Bogoliubov Laboratory for Theoretical Physics, Joint Institute for Nuclear Research, 141980 Dubna, Russia and
Center for Materials Theory, Department of Physics and Astronomy, Rutgers University, Piscataway, NJ 08854

(Dated: March 22, 2024)

The problem of importance of strong correlations for the electronic structure, transport and magnetic properties of half-metallic ferromagnetic CrO_2 is addressed by performing density functional electronic structure calculations in the local spin density approximation (LSDA) as well as using the LSDA+U method. It is shown that the corresponding low temperature experimental data are best fitted without accounting for the Hubbard U corrections. We conclude that the ordered phase of CrO_2 is weakly correlated.

PACS numbers: 71.27.+a, 75.30.Gw, 79.60.-i

As a compound with multiple industrial applications and its unusual half-metallic electronic structure, CrO_2 has recently attracted a lot of theoretical^{1,2,3,4,5,6} and experimental^{7,8,9,10,11} interest. The main discussion was centered around the role of strong correlations for the description of its ferromagnetic phase. Since Cr in its formal $4+$ valence state has two 3d electrons of t_{2g} symmetry, one would expect manifestation of correlation effects of the Mott-Hubbard nature. On the other hand, metallic behavior of spin majority band suggests that Coulomb interactions of the Hubbard type can be screened out³. The comparison with the available photoemission and optical conductivity data did not make the situation more clear. One-electron spectra calculated using the LSDA+U method^{12,13} as well as the photoemission and inverse photoemission experiments with the choice of intra-atomic Coulomb and exchange parameters $U = 3$ eV and $J = 0.87$ eV^{3,7}. This indicates the importance of strong correlations. Contrary to this result, the LSDA optical conductivity calculations explain experimental data⁴, which suggests the regime of weak coupling.

In the present paper we address the issue of controversial role of strong correlations in ferromagnetic CrO_2 by presenting combined studies of its electronic structure, optical conductivity and magnetic anisotropy using the LSDA and LSDA+U schemes. We employ a linear-muffin-tin-orbital (LMTO) method in its atomic sphere approximation (ASA)^{14,15} for our electronic structure calculations. The low symmetry of the rutile structure and small packing factor of the unit cell require an introduction of additional empty spheres. Their positions are chosen to be 4c and 4g in Wyckoff notations. The radii of the spheres (in atomic units) for Cr and O atoms, as well as of the empty spheres are chosen to be 1.975, 1.615, 1.378 and 1.434, correspondingly. The basis set adopted in the calculations is Cr(4s, 4p, 3d) and O(2s, 2p).

In rutile structure Cr atoms are surrounded by distorted oxygen octahedra. The positions of the octahedra lead to a new natural basis for Cr orbitals. In this basis the cubic component of the octahedral crystal field splits the fivefold degenerate 3d orbital into higher energy doubly degenerate e_g level and lower energy triple degenerate t_{2g} level. Distortions of oxygen octahedra further split the t_{2g} states into lower energy t_{2g}^k orbital (xy character) and higher energy twofold degenerate t_{2g}^2 orbitals (yz + zx and yz - zx characters)³.

The results of the LSDA band structure calculation in the vicinity of the Fermi energy are shown in Figs. 1 and 2. The Fermi level crosses the spin majority t_{2g} manifold. The rest of the Cr 3d states is formed from four e_g bands and three t_{2g} spin minority bands which are located above the Fermi level. In both spin channels e_g and t_{2g} bands are well separated for all momenta except for the Γ -point. The whole 3d complex is strongly hybridized with oxygen. In Fig. 2 one can see that in the spin minority channel there is gap of approximately 1.3 eV between the oxygen 2p band and the chromium d band. This gap leads to 100% spin polarization at E_F and assures the magnetic moment to be precisely equal to 4 μ_B per unit cell. The t_{2g} bands that cross the Fermi level in the spin majority channel mainly consist of the t_{2g}^2 orbitals (see Fig. 1). A most non-dispersive narrow band below E_F (shown as lightly shaded) is formed by the t_{2g}^k orbital. This localized state undergoes large exchange splitting^{ex} making spin minority t_{2g}^k orbitals unoccupied (see Fig. 2).

The main changes which occur in the band structure for non-zero values of U and J using the LSDA+U method are schematically shown in Fig. 3. These calculations were performed with $U = 3$ eV and $J = 0.87$ eV. The center of gravity of occupied t_{2g}^k band is pushed down by 0.6 eV. The spin minority unoccupied e_g bands are

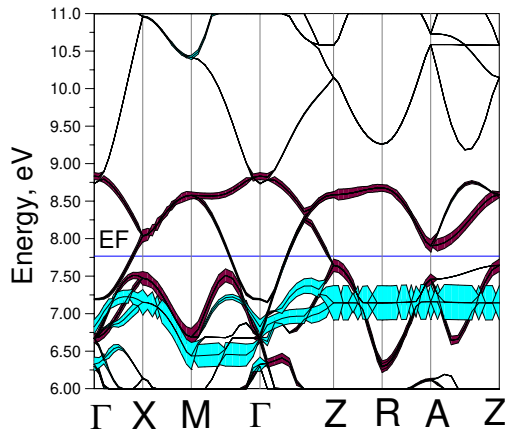


FIG. 1: LSDA band structure of CrO_2 for spin majority carriers. Dark and light shaded areas show the specific weight of t_{2g} and e_g orbitals respectively in the particular band.

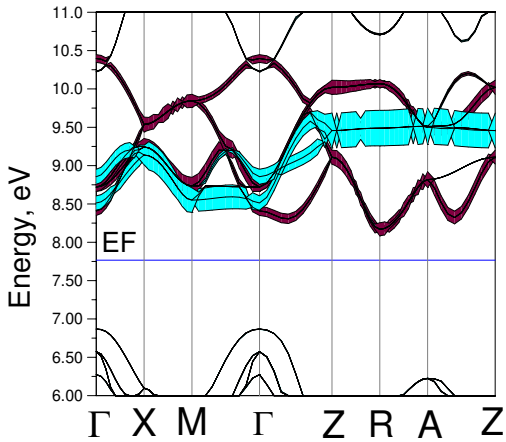


FIG. 2: LSDA band structure of CrO_2 for spin minority carriers. Dark and light shaded areas show the specific weight of t_{2g} and e_g orbitals respectively in the particular band.

pushed up by 0.6 eV, which opens 0.4 eV gap between t_{2g} and e_g bands above the Fermi level. In the spin minority channel the occupied oxygen bands are shifted up by 0.3 eV. The upper unoccupied t_{2g} and e_g bands are shifted up by 1.1 eV. As a result, the insulating gap is increased and reaches the value of 2.1 eV.

Now we compare our calculated electronic structure using the LSDA and the LSDA+U method with the available experimental data. Fig. 4 shows comparison of ultraviolet photoemission spectroscopy (UPS) experiments⁷ (photon energy $h\nu = 40.8$ eV) with the theoretical spectra which are calculated densities of states smeared by both Gaussian and Lorentzian broadening functions. The Gaussian broadening takes into account experimental resolution while Lorentzian takes into account finite lifetime effects. The Gaussian broadening parameter is taken to be 0.4 eV. The full width at half

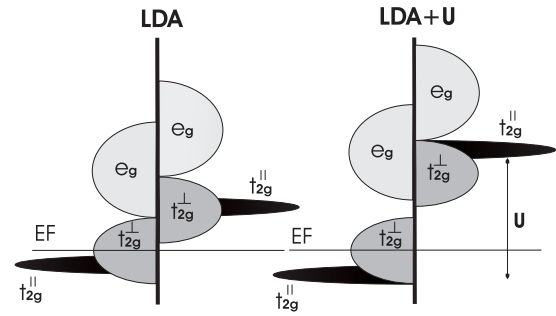


FIG. 3: Schematic density of states (DOS) of CrO_2 deduced from the LSDA and LSDA+U calculations. Shaded semicircles from right and left represent the bands for spin majority and spin minority carriers.

maximum (FWHM) of the Lorentzian was taken to be energy dependent and equal to $0.2(E - E_F)$ eV. We can distinguish two main features in the UPS spectra: (i) a small hump in around 1.5 eV which arises from the t_{2g} band of Cr, and (ii) a big hump around 6.0 eV which comes from the broad 2p oxygen band. Both features are fairly well described by both the LSDA and the LSDA+U calculation. The small discrepancy between the LSDA calculation and experiment could be referred to the fact that at small photon energies photoemission is a more surface sensitive technique. Indeed, recent PES studies of Vanadium oxides¹⁶ have been found to yield spectra not characteristic of the bulk, but rather of surface atoms whose lower coordination number can render more strongly correlated surface layer.

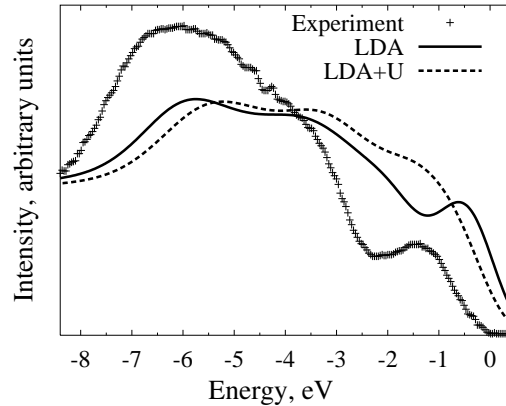


FIG. 4: Comparison between theoretical densities of states and experimental⁷ UPS spectra for CrO_2 . The theoretical DOS were smeared out by Gaussian and Lorentzian broadening functions to account for experimental resolution and lifetime effects. The secondary electron background has been taken into account.

For the unoccupied states we have chosen to compare our results with the available x-ray absorption spectra (XAS)¹¹ rather than with the inverse photoemission as it had been done before⁷. The main reason for this is

that XAS is a bulk (not surface) sensitive method. The 2p Cr XAS spectrum¹¹ is compared to our theoretical calculations in Fig. 5. To deduce theoretical spectra we performed both Gaussian and Lorentzian broadening of 3d and 4s partial DOSes. Two first peaks around 0.5 eV and around 1.5 eV come from the unoccupied 3d orbitals of chromium. The main contribution to the second peak comes from the t_{2g} orbitals in the spin minority channel. Thus, the LSDA + U overestimates the spin minority gap twice as much.

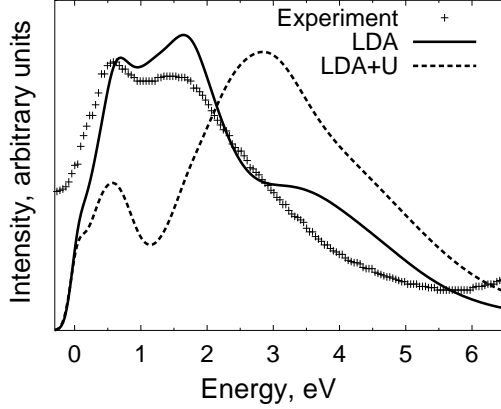


FIG. 5: Comparison between theory and experiment¹¹ for Cr 2p x-ray absorption (XAS) spectrum. To deduce theoretical curve from the partial Cr 3d DOS we used 0.1 eV for Gaussian FWHM. The Lorentzian FWHM was taken to be energy dependent and equal to $0.2(E - E_F)$. The binding energy of core $2p_{3/2}$ Cr state 577 eV has been subtracted from the experimental spectrum.

Below we discuss the optical conductivity of CrO_2 . In Fig. 6 diagonal x-components of the optical conductivity calculated using the LSDA and LSDA + U methods are compared with the experimental results reported by Basov and coworkers⁸ (x coordinate refers to the basis of unit cell). The main two features of the calculated optical conductivity are a shoulder around 2–3 eV and a broad hump located at energies 0.2–1.5 eV. In both LSDA and LSDA + U schemes the shoulder can be identified with two types of transitions. First contribution arises from the minority spin gap transitions and the second one comes from transitions between the occupied t_{2g}^k and unoccupied e_g bands. The hump is formed by interband transitions within the t_{2g} -manifold and the oxygen 2p bands near the Fermi level in the spin majority channel. Apparently, the LSDA prediction is much closer to the experimental curve than the LSDA + U one. The LSDA + U calculations overestimate the minority gap, and due to that, the spin minority transitions occur at higher energies.

Results of the calculated magnetic anisotropy of CrO_2 are presented below. Magnetic anisotropy is the dependence of internal energy on the direction of spontaneous magnetization. The magnetic anisotropy is a relativistic phenomenon arising due to spin-orbit coupling, where

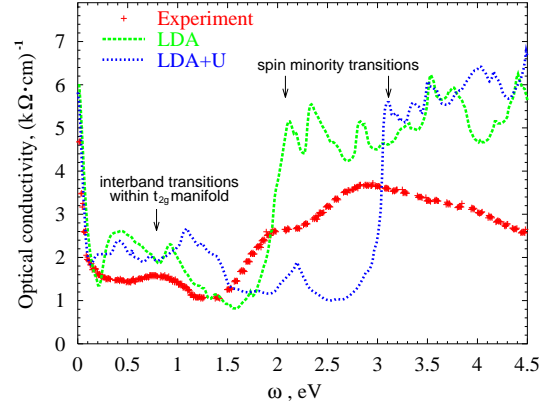


FIG. 6: Comparison of the optical conductivity of CrO_2 obtained using the LSDA and LSDA + U methods against the experimental data⁸.

the spin degrees of freedom interact with the spatial anisotropy through the coupling to the orbital degrees of freedom. This induces a preferred direction of spins. Because CrO_2 is a metastable compound, which irreversibly decomposes at about 200 °C, all measurements for this material are performed on polycrystals, microgranules or thin films. The first reliable result on magnetocrystalline anisotropy measurements was reported in Ref. 17. The discovery of the atmospheric pressure chemical vapor decomposition (CVD) technique has allowed to grow high-quality films of CrO_2 . As a result, in recent years a lot of studies of magnetic properties were performed on epitaxial CrO_2 layers deposited on single crystal (100) TiO_2 substrates^{18,19,20}. For thicker films (700 Å–1.2 μm) the in-plane magnetic anisotropy was observed with [001] and [010] easy and hard axis directions respectively. The magnetocrystalline anisotropy constant K_1 has been reported by different groups to be $4.4 \cdot 10^5 \text{ erg} \cdot \text{cm}^{-3}$ ²⁰, $2.7 \cdot 10^5 \text{ erg} \cdot \text{cm}^{-3}$ ¹⁹ and $1.9 \cdot 10^5 \text{ erg} \cdot \text{cm}^{-3}$ ¹⁸. However, these values can significantly differ from the bulk quantities because of a large lattice mismatch between CrO_2 films and TiO_2 substrates (till 4%). The relaxation as a function of thickness is very gradual and even for 1.2 μm film magnetic anisotropy shows significant deviation from the bulk value.

We calculate the magnetic anisotropy energy (MAE) by taking the difference of the two total energies with different directions of magnetization ([001], [010], [111] and [102]). For the momentum space integration, we follow the analysis given by Tryggvason and coworkers²¹ and use special point method²² with a Gaussian broadening²³ of 15 mRy. The validity and convergence of this procedure has been tested in their work²¹. We used about 1000 k-points in the irreducible Brillouin zone, while the convergence of MAE is tested up to 8000 k-points.

The direction [001] was found to be easy magnetization axis within our LSDA calculation which is consistent with latest thin film experiments^{18,19,20}. Numerical values of MAE in this case exceed the maximum experi-

mental value by approximately two times²⁰.

To figure out the influence of intra-atomic repulsion U on the magnetic anisotropy, we have performed LSDA + U calculations for different values of U increasing it from 0 to 6 eV ($J = 0.87$ eV has been kept constant except for the LSDA $U = 0$ case). The results of these calculations are presented in Fig. 7. MAE decreases rapidly starting from the LSDA value (which is approximately equal to 68 eV per cell) and changes its sign around $U = 0.9$ eV. This leads to switching correct easy magnetization axis [001] to the wrong one, namely [102]. The biggest experimental value of the MAE reported in the literature is 15.6 eV per cell²⁰. The calculated MAE approaches this value around $U = 0.6$ eV. This signals that correlation effects in the d -shell may be important for this compound although they are strongly screened out.

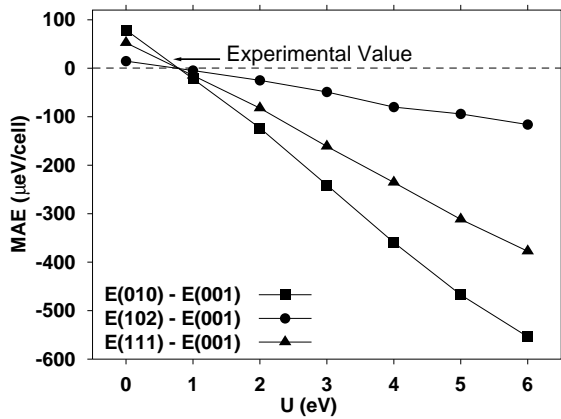


FIG. 7: The magneto-crystalline anisotropy energies for CrO_2 as functions of U . The experimental value of MAE $E[100] - E[001] = 15.6$ eV per cell is shown by arrow.

To conclude, we have reported the LSDA and

LSDA + U calculations of electronic structure, optical conductivity and magnetic anisotropy of CrO_2 . Our comparisons with the experimental data revealed that the best match is provided by the local spin density approximation. We explained the discrepancy between the LSDA and photoemission studies, discussed earlier by other authors^{3,7}, by the fact that due to small photon energies used in PES, it is more surface rather than bulk sensitive technique. We resolved this problem by showing that XAS spectrum is unambiguously described by the LSDA calculation. It has been also shown that even intermediate values of U (of the order of 1-2 eV) lead to the failure of the LSDA + U method to describe the magnetic anisotropy and the optical conductivity of CrO_2 . Since the LSDA + U is not adequate for the description of electronic structure of CrO_2 as well as of its optical and magnetic properties, we conclude that the ordered phase of CrO_2 could be described as weakly correlated material with small values of on-site Coulomb repulsion. It is important to notice that, while we have found that the simple one-electron picture describes well the ferromagnetic phase of this material, there is a narrow band formed by the non-dispersive t_{2g}^{jj} orbitals (xy character) which in the paramagnetic phase will be single occupied, due to the on-site Coulomb interactions, an effect which cannot be described in LDA and will require a Dynamical Mean-Field treatment for this materials as done in Ref. 5. The physical basis for the applicability of static mean-field picture in the ferromagnetic phase of this material, is due to the large exchange splitting which is able to effectively enforce the single occupancy of the t_{2g}^{jj} orbitals.

This research was supported by the ONR grant No. 4-2650. The authors would like to thank I. I. Mazin for helpful and enlightening discussions.

- ¹ K. Schwarz, J. Phys. F 16, L211 (1986).
- ² S. P. Lewis, P. B. Allen, and T. Sasaki, Phys. Rev. B 55, 10253 (1997).
- ³ M. A. Korotin, V. I. Anisimov, D. I. Khomskii, and G. A. Sawatzky, Phys. Rev. Lett. 80, 4305 (1998).
- ⁴ I. I. Mazin, D. J. Singh, and C. Ambrosch-Draxl, Phys. Rev. B 59, 411 (1999).
- ⁵ M. S. Laad, L. C. Raco, and E. Müller-Hartmann, Phys. Rev. B 64, 214421 (2001).
- ⁶ L. C. Raco, M. S. Laad, and E. Müller-Hartmann, Phys. Rev. Lett. 90, 237203 (2003).
- ⁷ T. Tsuchiya, T. Mizokawa, J. Okamoto, A. Fujimori, M. Nohara, H. Takagi, K. Yamaura, and M. Takano, Phys. Rev. B 56, R15509 (1997).
- ⁸ E. J. Singley, C. P. Weber, D. N. Basov, A. Barry, and J. M. D. Coey, Phys. Rev. B 60, 4126 (1999).
- ⁹ C. B. Stagarescu, X. Su, D. E. Eastman, K. N. Altmann, F. J. Himpsel, and A. Gupta, Phys. Rev. B 61, R9233 (2000).
- ¹⁰ J. Kunes, P. Novak, P. M. Oppeneer, C. Konig, M. Fraune, U. Rudiger, G. Guntherodt, and C. Ambrosch-Draxl, Phys. Rev. B 65, 165105 (2002).
- ¹¹ E. Z. Kurnev, A. Moewes, S. M. Butorin, M. I. Katsnelson, L. D. Finkelstein, J. Nordgren, and P. M. Tedrow, Phys. Rev. B 67, 155105 (2003).
- ¹² V. I. Anisimov, F. Aryastawan, and A. I. Lichtenstein, J. Phys.: Condensed Matter 9, 767 (1997).
- ¹³ For a review, see, e.g., Strong Correlations in electronic structure calculations, edited by V. I. Anisimov (Gordon and Breach Science Publishers, Amsterdam, 2000).
- ¹⁴ O. K. Andersen, Phys. Rev. B 12, 3060 (1975).
- ¹⁵ S. Y. Savrasov, Phys. Rev. B 54, 16470 (1996).
- ¹⁶ S.-K. Mo, J. D. Denlinger, H.-D. Kim, J.-H. Park, J. W. Allen, A. Sekiyama, A. Yamasaki, K. Kadohira, S. Suga, Y. Saitoh, T. Muro, P. Metcalfe, G. Keller, K. Held, V. Eyert, V. I. Anisimov, and D. Vollhardt, Phys. Rev. Lett. 90, 186403 (2003).
- ¹⁷ W. H. Cloud, D. S. Schreiber, and K. R. Babcock, and J. Appl. Phys. 33, 1193 (1962).
- ¹⁸ L. Spinu, H. Srikanth, A. Gupta, X. W. Li, and Gang Xiao, Phys. Rev. B 62, 8931 (2000).

- ¹⁹ F. Y. Yang, C. L. Chien, E. F. Ferrari, X. W. Li, Gang Xiao, and A. Gupta, Appl. Phys. Lett. 77, 286 (2000).
- ²⁰ X. W. Li, A. Gupta, and Gang Xiao, Appl. Phys. Lett. 75, 713 (1999).
- ²¹ J. Trygg, B. Johansson, O. Eriksson, and J. M. Wills, Phys. Rev. Lett. 75, 2871 (1995).
- ²² S. Froyen, Phys. Rev. B 39 3168 (1989).
- ²³ M. Methfessel and A. T. Paxton, Phys. Rev. B 40, 3616 (1989).